Romanian Reports in Physics, Vol. 59, No. 2, P. 411–417, 2007

Dedicated to Prof. Dorin N. Poenaru's 70th Anniversary

PROBING NUCLEAR MEAN FIELD BY PROTON EMISSION

D.S. DELION[1], R.J. LIOTTA[2]

[1] *National Institute of Physics and Nuclear Engineering POB MG-6, Bucharest-Măgurele, Romania*

[2] *KTH, Alba Nova University Center, SE-10691 Stockholm, Sweden*

(Received January 10, 2007)

Abstract. We show that proton emission is a valuable tool to investigate mean field properties of exotic proton rich nuclei. We give a formula that relates the logarithm of the half-life, corrected by the centrifugal barrier, with the Somerfeld parameter in proton decay processes. The corresponding experimental data lie on two straigth lines which appear as a result of a sudden change in the nuclear shape, marking two regions of deformation. This feature provides a powerfull tool to assign experimentally quantum numbers and deformations in proton emitters.

Key words: proton emission, half-life, Coulomb function, angular momentum.

Nowadays the challenge in nuclear physics is related to rare nuclei, i.e. nuclei lying very far from the stability line which decay rapidly by particle emission (neutron and proton drip lines) [1]. The exploration of the drip-lines is one of the ambitions of the projected radioactive nuclear bean facilities as e.g. the Rare Isotope Accelator (RIA) [2, 3].

By plotting the logarithm of the half-lives as a function of Q_p, i.e. the kinetic energy of the emitted proton, one does not obtain a clear graphical pattern of the experimental data, as in the Geiger-Nutall rule. As seen in Fig. 1.a [4], such a plot does not show any obvious trend. The reason of this disorder is that not only Q_p but also the height and width of the Coulomb and centrifugal barriers, in which the proton is trapped before decaying, determine the decay width. Or, in other words, it is the probability of penetration through the total barrier that determines the decay. Assuming that the proton is located at a point R, the half-life corresponding to that wave, with given

angular momentum and total spin (l,j), can be written as [5]

$$T_{1/2}=\frac{\ln 2}{v}\left|\frac{H_l^{(+)}(\chi,\rho)}{s_{lj}(R,\beta)}\right|^2, \tag{1}$$

where $H_l^{(+)}$ is the Coulomb-Hankel spherical wave, $\chi=2(Z-1)e^2/(\hbar v)$ is the Somerfeld parameter, which determines the Coulomb barrier, Z is the charge number of the mother nucleus, $v=\hbar k/\mu=\sqrt{2Q_p/\mu}$ is the asymptotic velocity of the outgoing proton, μ is the reduced mass of the proton-daughter system, $\rho=kR$ and the spectroscopic function is given by [6]

$$s_{lj}(R,\beta)=\sum_{l'j'}K_{lj;l'j'}(R,\beta)s^{(0)}_{l'j'}f_{l'j'}(R,\beta), \tag{2}$$

where $s^{(0)}_{lj}$ is the so-called spectroscopic factor (the particle probability u^2_{lj} within the superfluid model) and f_{lj} are the components of the internal wave function (the standard Nilsson function within the adiabatic approach). The asymptotic propagator matrix is given by [6]

$$K_{lj;l'j'}(R,\beta)\equiv H_l^{(+)}(\chi,\rho)\left[\mathcal{H}^{(+)}(R,\beta)\right]^{-1}_{lj;l'j'}=\delta_{ll'}\delta_{jj'}+\Delta K_{lj;l'j'}(R,\beta). \tag{3}$$

Here $\mathcal{H}^{(+)}_{lj;l'j'}(R,\beta)$ is the matrix of solutions with an outgoing boundary behavior, i.e. $\mathcal{H}^{(+)}_{lj;l'j'}(R,\beta)\rightarrow_{R\rightarrow\infty}\delta_{ll'}\delta_{jj'}H_l^{(+)}(\chi,\rho)$. It is fully determined by the concrete form of the interaction. Thus, the relation (1) has the same form as in the spherical case, but for deformed systems the spectroscopic function is a superposition of the different channel components f_{lj}. Our coupled channels calculations showed that, even for the most deformed emitter ^{131}Eu with $\beta=0.33$, the nondiagonal contribution is relative small, i.e. $\max(\Delta K)<0.1$, for distances at which the nuclear part of the interaction has vanishing values.

The ratio $H_l^{(+)}/s_{lj}$, entering Eq. (1) (which is just the inverse of the scattering amplitude in the (l,j) channel) does not depend upon the radius and this is an important test of accuracy in any coupled channels scheme. A good approximation of the Coulomb-Hankel function $H_l^{(+)}$ for energies involved in proton emission is given by the WKB value, i.e. [5]

$$H_l^{(+)}(\chi,\rho)\approx C_l(\chi,\rho)(\mathrm{ctg}\,\alpha)^{1/2}\exp[\chi(\alpha-\sin\alpha\cos\alpha)]. \tag{4}$$

The influence of the centrifugal barrier is fully contained in the function C_l

$$C_l(\chi,\rho)=\exp\left[\frac{l(l+1)}{\chi}\,\mathrm{tg}\,\alpha\right],\quad \cos^2\alpha=\frac{Q_p}{V_c(R)}=\frac{\rho}{\chi}, \tag{5}$$

where $V_c(R)$ is the Coulomb potential at distance R. We will choose this distance as the matching radius, for which we will adopt the standard form, i.e.

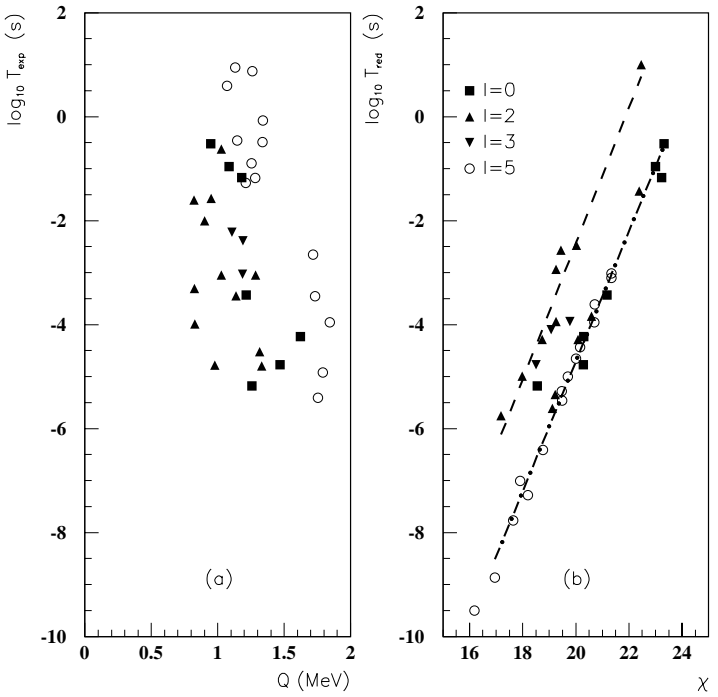

Fig. 1 – a) Logarithm of the experimental half-lives corresponding to proton decay as a function of the Q-value. The data are taken from Ref. [4]; b) values of $\log_{10}\ T_{red}$, Eq. (6), as a function of the Coulomb parameter χ, The numbers labelling the different symbols correspond to the l-values of the outgoing proton. The two lines are computed according to Eq. (8).

$R = 1.2(A_d^{1/3} + A_p^{1/3})$, where A_d is the mass number of the daughter nucleus and $A_p = 1$. The dependence of the centrifugal factor upon the distance, entering through α, is very weak around that value of R. Defining a reduced half-life as

$$T_{red} = \frac{T_{1/2}}{C_l^2} = \frac{F(\chi,\rho)}{|s_{lj}(R,\beta)|^2}, \tag{6}$$

where

$$F(\chi,\rho) = \frac{\ln 2}{v}\,\mathrm{ctg}\,\alpha \exp[2\chi(\alpha - \sin\alpha\cos\alpha)], \tag{7}$$

one sees that T_{red} should not depend upon the angular momentum l if plotted against the dimensionless Coulomb parameter χ. Moreover, $\log_{10}\ T_{red}$ which, according to Eq. (7), is proportional to $2\chi(\alpha - \sin\alpha\cos\alpha)$, is a linear function of χ independently of the value of l, provided the velocity v, the function s_{lj} and the parameter α, which depend upon the Q-value, has a smooth behaviour in this logarithmic scale. Notice that the value of T_{red} is model independent since the only theoretical quantity entering in its definition is the function C_l^2,

which is a by-product of the barrier penetration process. But it is important to stress that this entire analysis is based upon the assumption that the proper value of l, that is the one that determines the experimental half-life $T_{1/2}$, is used. Otherwise, and since $T_{1/2}$ is strongly l-dependent, that straight line pattern would be completely spoiled.

To check the rather straightforward conclusions reached above we evaluated $\log_{10}\ T_{red}$ in cases where experimental data are available, as shown in Table 1 of the reference [7]. We considered proton emitters with $Z > 50$ and angular momentum as given in Ref. [4]. The value of the proton angular momentum l outside the nucleus is extracted from theoretical predictions.

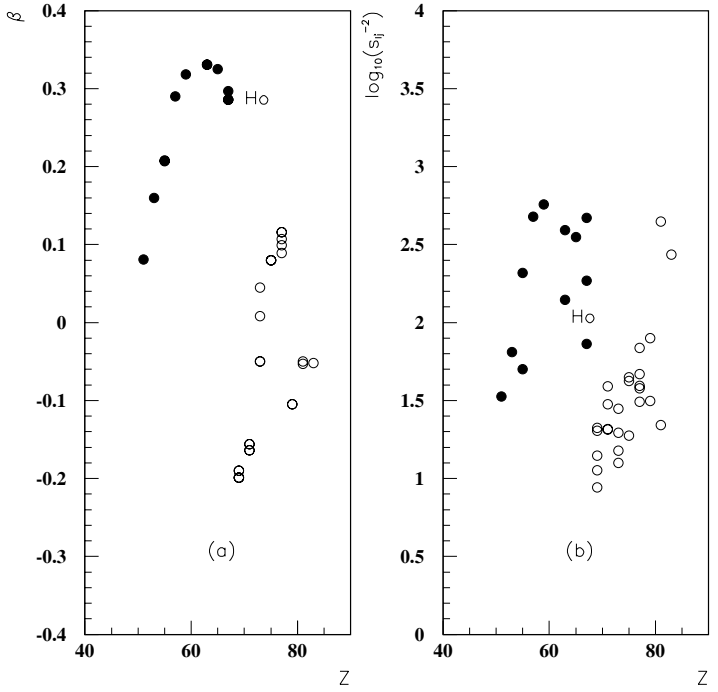

Fig. 2 – a) Dependence of the quadrupole deformation parameter β upon the charge number Z. Dark circles correspond to nuclei with $Z < 68$. Notice that β is the same in this scale for the isotopes C_s and also for the two states in H_o; b) the logarithm of the spectroscopic function s_{lj}^{-2}, defined by Eq. (1), *versus* the charge number Z.

With the values of l, χ and $\log_{10}\ T_{red}$ of we produced the plot shown in Fig. 1.b. Amazingly enough, the points lie all approximately along two straight lines. The nuclei on the upper line correspond to the emittrs with $Z < 68$. Using a fitting procedure we found that the experimental half-lives

can be reproduced by the formula

$$\begin{aligned} \log_{10}\ T_{red}^{(k)} &= a_k(\chi - 20) + b_k, \\ a_1 &= 1.31,\ b_1 = -2.44,\ Z < 68 \\ a_2 &= 1.25,\ b_2 = -4.71,\ Z > 68, \end{aligned} \tag{8}$$

where $k = 1$ corresponds to the upper line in Fig. 1.b. The standard errors are $\sigma_1 = 0.26$ and $\sigma_2 = 0.23$, corresponding to a mean factor less than two.

These two straight lines may have been induced either by a brusque change in the Q-values or in the structure of the different emitters, or by both. The Q-value dependence affects only the function $F(\chi, \rho)$, but our analysis showed that the two lines cannot be explained in this way. This forces us to conclude that although there is a change in the Q-values at $Z = 65$ (which can also be seen by plotting the dependence of ρ versus Z), this effect can not be the only reason behind the two straight lines of Fig. 1.b. The only other source that may contribute to that alignment is an abrupt change in the nuclear structure of the emitters. We therefore correlated the deformation values calculated in Ref. [8] with the determined half-lives.

In Fig. 2.a we show the deformation parameter β as a function of Z. At the proton drip line between $Z = 67$ and $Z = 69$ occurs a pronounced change, from a large prolate shape with $\beta \approx 0.3$ to an oblate shape with $\beta \approx -0.2$. These shapes are substantiated by measurements of moments of inertia. In order to analyse the dependence of the half-life upon the internal structure of the nucleus we plot in Fig. 2.b the quantity s_{lj}^{-2} as a function of the charge number Z. It is worthwhile to emphasize once again that this is a model independent function.

One remarks a striking correlation between Figs. 2.a and 2.b. After the jump occurrying at $Z = 68$, where a brusque shape change occurs, the deformation of the nuclei lying on the lower line smoothly increases. One can then assert that these lines reflect two regions of nuclei separated by a sharp transition between the prolate and oblate regimes.

Moreover, if one represents the dependence of s_{lj}^{-2} versus β one obtains the distribution in Fig. 3, which is clearly clustered around the two dashed lines. In one uses this linear dependence for s_{lj}^{-2} as a function of β to estimate the half-lives one obtains exactly the two lines in Fig. 1.b.

There is a point in Fig. 1.b that deviates conspicuosly from the upper straight line. That is the solid square corresponding to ^{141}Ho*. In Fig. 2 a one sees that this nucleus is situated at the border between the two regions of deformation, which is consistent with the interpretation given here to the behaviour of $\log_{10}\ T_{red}$ since the decay proceeds in this case from an excited state. Therefore not only the deformation but also nuclear structure effects,

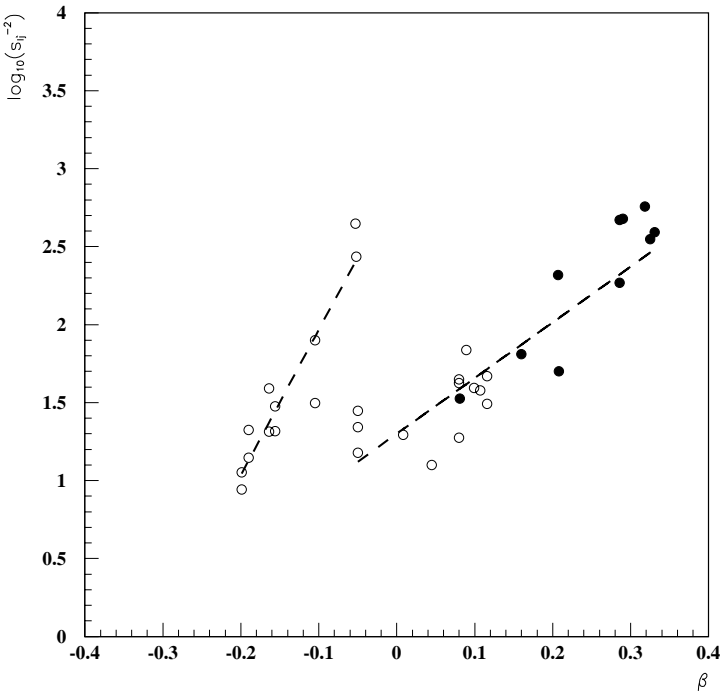

Fig. 3 – The logarithm of the spectroscopic function s_{lj}^{-2}, defined by Eq. (1), versus the quadrupole deformation parameter β.

absent in the adjacent nuclei, become important, as can be seen by comparing Figs. 2.a with 2.b.

The remarkable agreement between the data and the straight lines behaviour shown in Fig. 1.b can hardly be considered accidental. Will all nuclei lie on these two lines or will another region in the nuclear chart occur, with yet another line? These are important questions to answer and we encourage further experimental efforts directed to the measurement of half-lives and Q-values in proton decays.

In conclusion we have shown in this paper that the proton half-lives are strongly correlated with the nuclear shapes. The simple formula for proton decay (Eq. (8)) is the equivalent of the Geiger-Nutall rule. This formula allows one to assign presicely the spin and parity of proton decaying states. The only quantities that are needed are the half-life of the mother nucleus and the proton Q-value. As a function of these quantities, corrected by the centrifugal barrier (Eq. (6)), the experimental data lie along two straight lines. Since the decay probability is strongly dependent upon the orbital angular momentum l of the decaying proton, only properly assigned l-values will fit into those straight lines. Moreover, these two lines appear as a result of a sudden change

in the nuclear shape marking two regions of deformation. This can, therefore, be a powerful tool to determine experimentally quantum numbers as well as deformations in rare nuclei.

REFERENCES

1. P.J. Woods and C.N. Davids, Ann. Rev. Nucl. Part. Sci., **47**, 541 (1997).
2. ∗ ∗ ∗, *Rare isotope accelerator*, Argonne web page, `www.anl.gov/ria`
3. ∗ ∗ ∗, *Rare isotope accelerator* (RIA), NSCL web page, `www.nscl.msu.edu/ria`
4. A.A. Sonzogni, Nucl. Data Sheets, **95**, 1 (2002).
5. P. O. Fröman, Mat. Fys. Skr. Dan. Vid. Selsk., **1**, *3*, 1 (1957).
6. D.S. Delion, R.J. Liotta, and R. Wyss, Phys. Rep., **424**, 113 (2006).
7. D.S. Delion, R.J. Liotta, and R. Wyss, Phys. Rev. Lett., **96**, 072501 (2006).
8. P. Möller, R.J. Nix, W.D. Myers, and W. Swiatecki, At. Data Nucl. Data Tables, **66**, 131 (1995).